



Scientific Imaging Solutions for Light & Color Measurement

ProMetric® Imaging Colorimeters and Photometers are designed and calibrated around standard principles of light measurement to ensure quality for displays, light sources, and backlit components.

- Measure light & color based on **human visual perception**
- Imaging up to **61MP resolution**
- For use in **R&D labs** or fully automated **production lines**

**WATCH A VIDEO: RADIANT
CUSTOMER TESTIMONIAL** ▶



RADIANT
VISION SYSTEMS

Solution-processed high-performance organic light-emitting diodes containing a green-emitting multiresonant thermally activated delayed fluorescent dendrimer

Sen Wu | Dianming Sun, SID Member | Eli Zysmanl-Colman, SID Member 

Organic Semiconductor Centre,
EaStCHEM School of Chemistry,
University of St Andrews, St Andrews, UK

Correspondence

Dianming Sun and Eli Zysmanl-Colman,
Organic Semiconductor Centre,
EaStCHEM School of Chemistry,
University of St Andrews, St Andrews
KY16 9ST, UK.
Email: sd235@st-andrews.ac.uk and
eli.zysman-colman@st-andrews.ac.uk

Funding information

China Scholarship Council, Grant/Award
Number: 201906250199; Royal Academy
of Engineering, Grant/Award Number:
EF2122-13106; Engineering and Physical
Sciences Research Council, Grant/Award
Numbers: EP/L017008, EP/P010482/1

Abstract

A multi-resonance thermally activated delayed fluorescence (MR-TADF) dendrimer emitter and a related reference MR-TADF compound were designed, synthesized, and characterized for use as narrowband emitters in solution-processed OLEDs. The 1 wt% doped films in PMMA film revealed that the compounds **MR-D1** and **MR-D2** showed narrowband green emission at λ_{PL} of 490 and 495 nm and with FWHM of 23 and 29 nm, respectively. The 50 wt% doped films in mCP still show narrowband green emission at λ_{PL} of 495 and 499 nm and with FWHM of 28 nm for **MR-D1** and **MR-D2**, respectively, while conserving the small ΔE_{ST} of 0.14 and 0.13 eV, respectively. OLEDs containing an emissive layer consisting of 50 wt% **MR-D1** and **MR-D2** in mCP showed high EQE_{max} of 27.7% and 21.0%, respectively, and low efficiency roll-off of 19% and 30% at a luminance of 2000 cd/m⁻².

KEYWORDS

dendrimers, multiresonant thermally activated delayed fluorescence, solution-processed organic light-emitting diodes

1 | INTRODUCTION

Organic light-emitting diodes (OLEDs) are now widely used as the display technology in electronic devices such as mobile phones, smartwatches, and televisions. This is because OLEDs possess a desirable suite of properties that make them ideal for the displays such as providing deep color saturation, then can be viewed, even at obtuse viewing angles, they can show pure black, they can be fabricated on myriad substrates, permitting access to flexible, foldable and transparent displays.^{1–3} Almost all commercial OLEDs are fabricated using vacuum deposition. This fabrication technology is materials wasteful, where only 20% of the materials get

incorporated into the film during the film deposition.⁴ Solution-processing techniques, such as ink-jet printing, are an alternative technology that can lead to significant cost savings during the production of the device.⁵

Small molecule emitter materials, which are ideally suited for vacuum-deposited OLEDs, are not well suited for solution-processed OLEDs as film quality is poor and the morphological stability is low.⁶ Polymer emitters materials are a good option for solution-processed OLEDs because the polymer can form homogeneously smooth films; however, polymers come as a mixture of different weight materials, which makes them not ideal for this application. Dendrimers are ideal candidates for use in solution-processed OLEDs as the films formed are

This is an open access article under the terms of the [Creative Commons Attribution](https://creativecommons.org/licenses/by/4.0/) License, which permits use, distribution and reproduction in any medium, provided the original work is properly cited.

© 2023 The Authors. *Journal of the Society for Information Display* published by Wiley Periodicals LLC on behalf of Society for Information Display.

homogeneously smooth and the dendrimers can be obtained pure, just like small molecule emitters.⁷

Like phosphorescent complexes, thermally activated delayed fluorescence (TADF) emitters can efficiently harvest both triplet and singlet excitons to produce high-efficiency OLEDs. TADF works by upconverting triplet excitons into singlets by reverse intersystem crossing (RISC) in materials where there is a very small singlet-triplet energy gap, ΔE_{ST} .⁸⁻⁹ The most commonly used design employed is based on a twisted donor-acceptor architecture. For dendrimers, this manifests in the use of one or more donor dendrons attached to a central acceptor moiety.^{7,10} We previously reported high-performance solution-processed OLEDs using triazine-based dendrimer emitters that showed high maximum external quantum efficiencies (EQE_{max}) of 28.4%.⁷ Despite the high EQE_{max} and the low efficiency roll-off, the electroluminescence spectrum is very broad, which adversely impacts the color purity of the device.¹¹

Multiresonant TADF (MR-TADF) emitters are a subclass of TADF emitters and are based on polycyclic aromatic compounds that are both p- and n-doped. Their rigid structure endows these compounds with very narrowband emission, small Stokes shifts, and high radiative decay rates, which translate into bright devices of high color purity.¹²⁻¹³ MR-TADF compounds emit from a short-range charge transfer (SRCT) state and typically show moderate ΔE_{ST} . Here, we combine the merits from both dendrimer and MR-TADF emitters in the design of one of the first MR-TADF dendrimers (**MR-D1**), and we cross-compare its performance with the control emitter (**MR-D2**). Employing this strategy, host-free solution-processed OLEDs with **MR-D1** exhibit both a high EQE_{max} of 27.7% but also narrowband sky-blue EL at λ_{EL} of 493 nm with full width at half maximum (FWHM) of 27 nm. The device employing the control compound **MR-D2** as the emitter shows an EQE_{max} of 21.0% and λ_{EL} of 496 nm with FWHM of 27 nm.

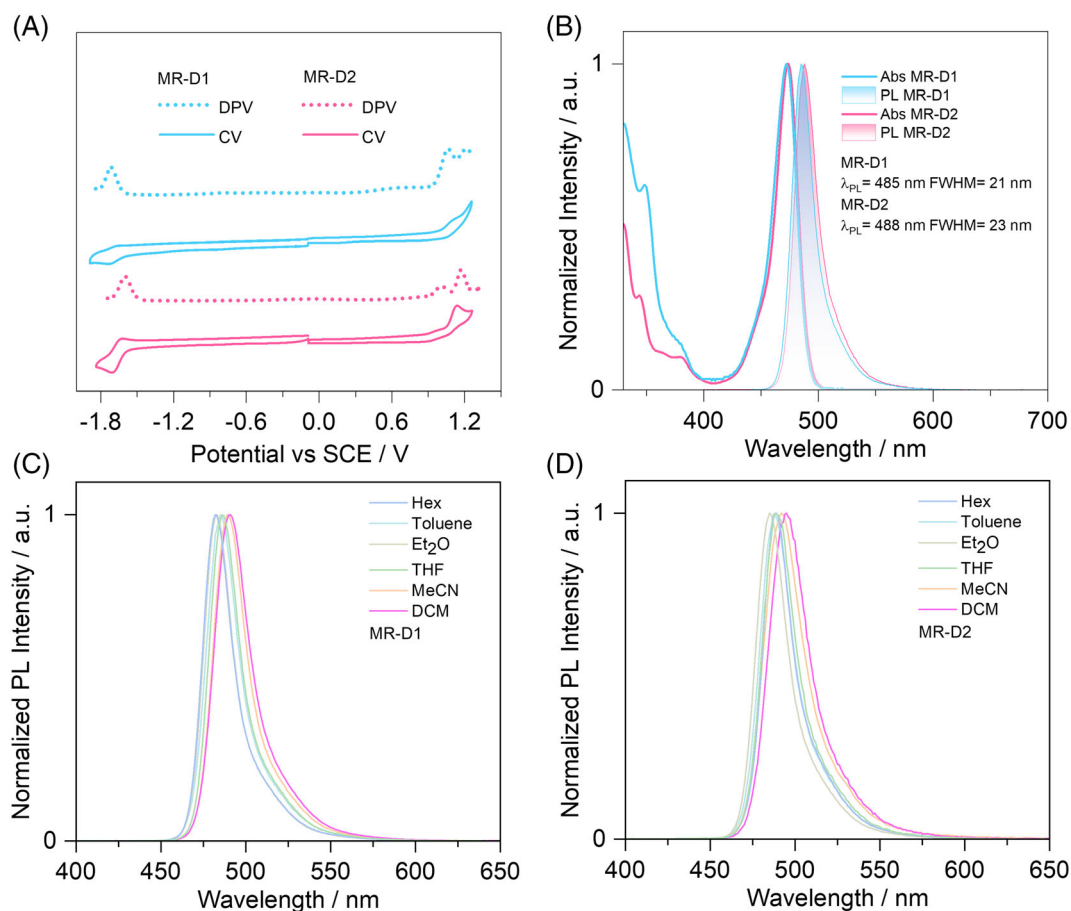


FIGURE 1 (A) Cyclic voltammogram (CV) and differential pulse voltammetry (DPV) of **MR-D1** and **MR-D2** in degassed DMF with 0.1 M [ⁿBu₄N]PF₆ as the supporting electrolyte and Fc/Fc⁺ as the internal reference (0.45 V vs. SCE).¹⁴ (B) Absorption and steady-state PL spectra (SS) of **MR-D1** and **MR-D2** in dilute toluene at room temperature ($\lambda_{exc} = 340$ nm). Solvatochromatic PL study of (C) **MR-D1** and (D) **MR-D2** ($\lambda_{exc} = 340$ nm).

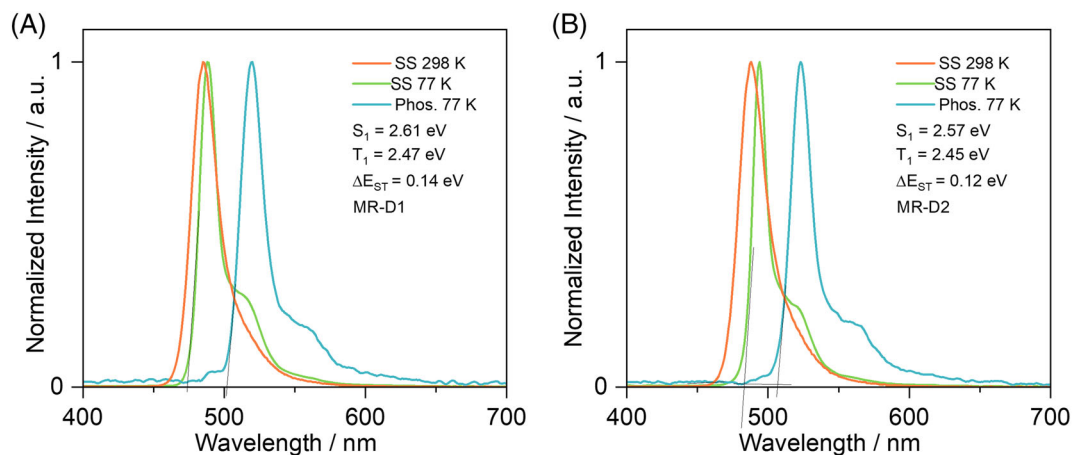


FIGURE 2 Steady-state PL (298 and 77 K) and phosphorescence spectra (1–10 ms, 77 K) of (A) **MR-D1** and (B) **MR-D2** in toluene ($\lambda_{exc} = 340$ nm).

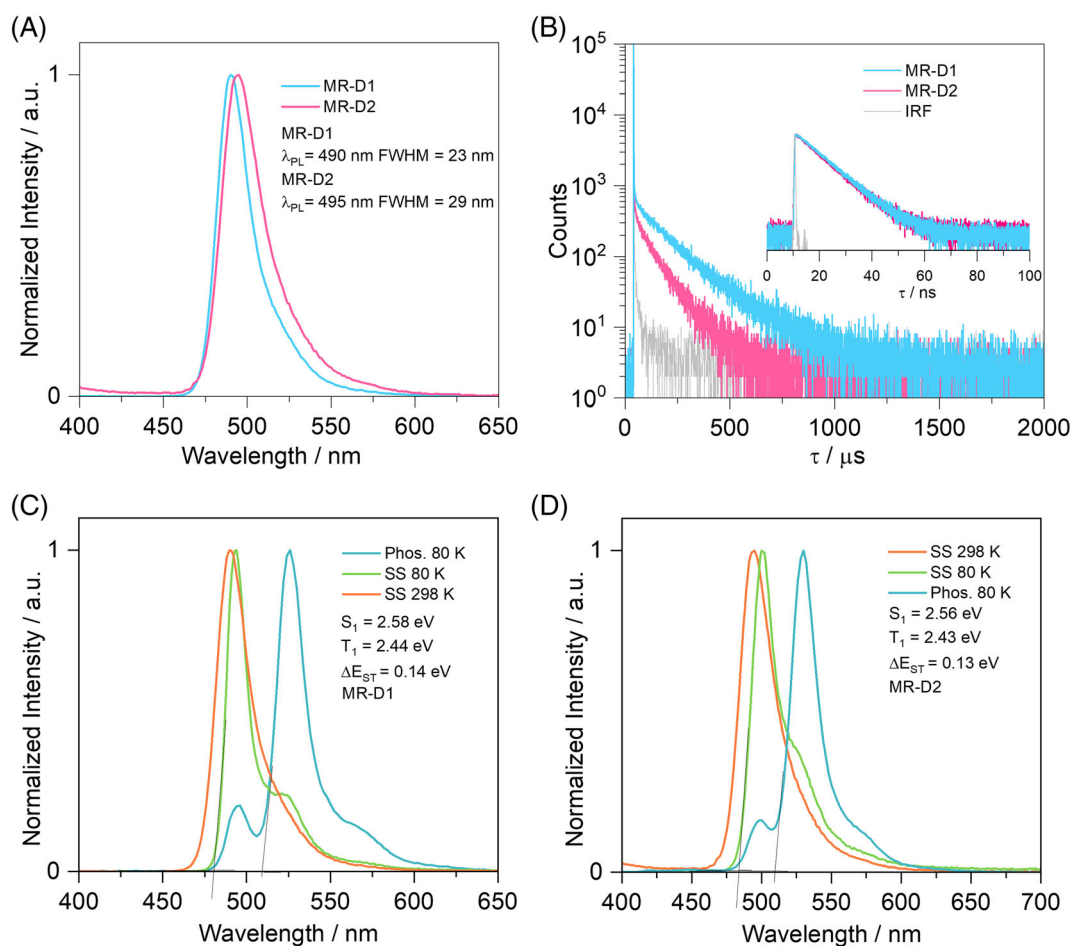


FIGURE 3 (A) Steady-state PL of **MR-D1** and **MR-D2** in 1 wt% PMMA film ($\lambda_{exc} = 340$ nm). (B) Time-resolved PL decay ($\lambda_{exc} = 375$ nm) in 1 wt% PMMA matrix; Steady-state PL (298 and 80 K) and phosphorescence spectra (80 K, 1–9 ms) of (C) **MR-D1** and (D) **MR-D2** in 1 wt% PMMA film ($\lambda_{exc} = 340$ nm).

2 | RESULTS AND DISCUSSION

Figure 1A shows the cyclic voltammetry (CV) and differential pulse voltammetry (DPV) scans in DMF, referenced versus SCE,¹⁴ of **MR-D1** and **MR-D2**. The compounds show reversible reduction waves at -1.73 and -1.61 V, respectively, and irreversible oxidation waves at 1.06 and 1.01 V, respectively. The corresponding HOMO/LUMO values are $(-5.40/-2.61$ eV) and $(-5.35/-2.73$ eV), leading to a HOMO-LUMO gap of 2.79 and 2.59 eV, for **MR-D1** and **MR-D2**, respectively. The UV-vis absorption and fluorescence spectra of **MR-D1** and **MR-D2** in dilute toluene solution are shown in Figure 1B. The absorption spectra show two distinct families of bands. The high-energy bands below 400 nm are from the π - π^* transition over the whole molecule and the low-energy bands beyond 400 nm are tentatively assigned to the SRCT transition states. The room temperature steady-state PL of **MR-D1** and **MR-D2** are narrowband and show peak emission, λ_{PL} , at 485 and 488 nm and FWHM of 21 and 23 nm, respectively. The red-shifted emission of **MR-D2** compared to **MR-D1** is consistent

with the smaller HOMO-LUMO gap observed in the electrochemistry. The narrowband emission and the corresponding small Stokes shift of 13 and 14 nm for **MR-D1** and **MR-D2** imply a very small geometry relaxation in the singlet excited state. This and the modest positive solvatochromism (Figure 1C-D) are characteristic of an emissive state of SRCT character and are hallmarks of MR-TADF emitters.

The ΔE_{ST} , calculated from the onsets of the steady-state fluorescence and delayed emission spectra at 77 K (Figure 2), are 0.14 and 0.12 eV for **MR-D1** and **MR-D2**, respectively, which are of comparable magnitude to other MR-TADF compounds such as **DOBONA** and **DABNA-1**.¹⁵

We next proceeded to explore the photophysical properties of **MR-D1** and **MR-D2** in the solid state as 1 wt% doped films in poly(methyl methacrylate) (PMMA). At this low doping level, we ensure that the photophysics reflects the single molecule and intermolecular interactions can be neglected. The steady-state PL spectra of **MR-D1** and **MR-D2** (at 298 K) show narrowband emission with FWHM of 23 and 29 nm at λ_{PL} of 490 and

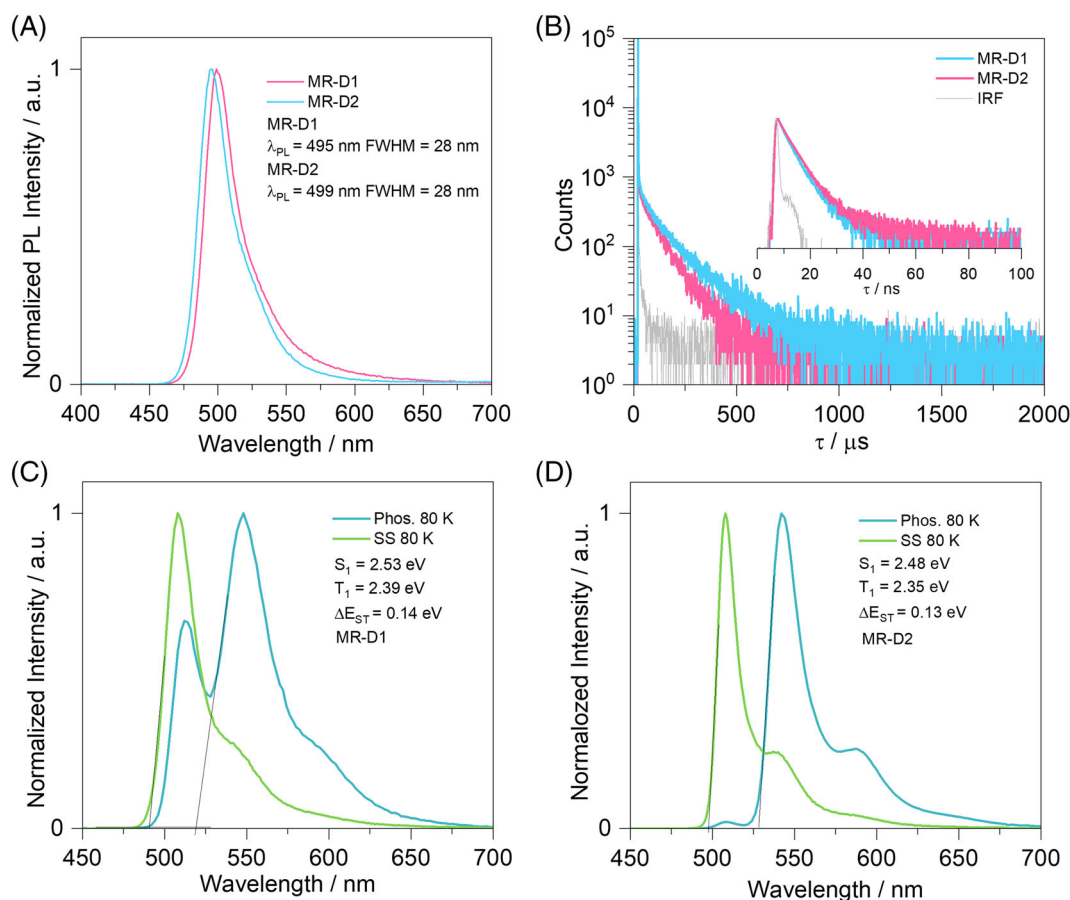


FIGURE 4 (A) Steady-state PL of **MR-D1** and **MR-D2** in 50 wt% mCP film ($\lambda_{\text{exc}} = 340$ nm). (B) Time-resolved PL decay ($\lambda_{\text{exc}} = 375$ nm) in 50 wt% mCP film; Steady-state PL (298 and 80 K) and phosphorescence spectra (80 K, 1–9 ms) of (C) **MR-D1** and (D) **MR-D2** in 50 wt% mCP MMA film ($\lambda_{\text{exc}} = 340$ nm).

495 nm, respectively. These values are identical to those observed in toluene solution (Figure 3A). The relatively narrower and blue-shift emission of **MR-D1** in PMMA film is consistent with that in toluene solution. The S_1 energy was inferred from the high-energy onset of the steady-state PL at 77 K to be 2.58 and 2.56 eV for **MR-D1** and **MR-D2**, respectively, while the T_1 energy was determined from the onset of the time-gated phosphorescence at 77 K to be 2.44 and 2.43 eV, respectively (Figure 3B–C). The corresponding ΔE_{ST} values are 0.14 and 0.13 eV for **MR-D1** and **MR-D2**, respectively, which are identical to the values obtained in toluene. Both compounds show biexponential decay kinetics with prompt lifetimes, τ_p , of 8.3 and 8.1 ns, and delayed lifetimes, τ_d , of 159 and 91 μ s for **MR-D1** and **MR-D2**, respectively.

The studies in PMMA revealed the promise of these dendrimers as bright TADF compounds. We next studied to what degree of concentration quenching would exist in much more concentrated films. 1,3-Bis(*N*-carbazolyl)benzene (mCP) was identified as the best host material for these two dendrimers because of its suitably aligned energy levels with the adjacent layers in the OLED stack and the high-quality and homogeneous films that could

be prepared by spin-coating. The photoluminescence quantum yield was found to be the highest at 50 wt% in mCP. The photophysical properties of the 50 wt% doped films in mCP film are shown in Figure 4. The SS emissions of the 50 wt% doped film in mCP are narrow at λ_{PL} of 495 and 499 nm and having the same FWHM of 28 nm for **MR-D1** and **MR-D2**, respectively. The emissions for **MR-D1** and **MR-D2** only show a slight red-shift and almost the same emission profile compared to those in the 1 wt% doped film in PMMA (λ_{PL} of 490 and 495 nm with FWHM of 23 and 29 nm for **MR-D1** and **MR-D2**, respectively) indicating that the donor dendron can effectively suppress aggregation at the higher doping concentration. The corresponding ΔE_{ST} values are 0.14 and 0.13 eV for **MR-D1** and **MR-D2**, respectively, which are identical to the values obtained in both the PMMA film and toluene solution. Both compounds show biexponential decay kinetics with prompt lifetimes, τ_p , of 2.8 and 3.3 ns, and delayed lifetimes, τ_d , of 128.3 and 86.0 μ s for **MR-D1** and **MR-D2**, respectively.

Based on the promising photophysical properties of the emitters in the doped mCP films, simple bilayer devices consisting of ITO/PEDOT:PSS (35 nm)/mCP:

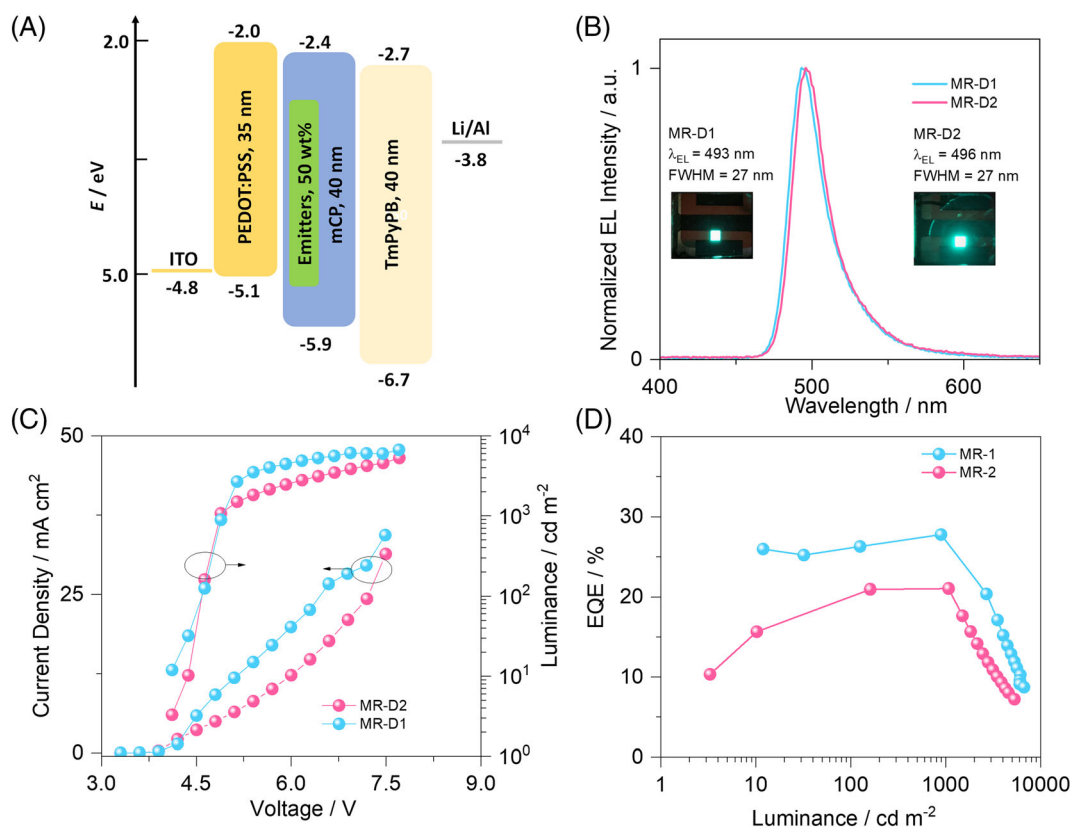


FIGURE 5 Electroluminescence characteristics of the OLED based on MR-D1 (Device 1) and MR-D2 (Device 2). (A) Device configuration. (B) Normalized electroluminescence spectra. (C) Current efficiency and power efficiency versus current density. (D) EQE versus brightness.

50 wt% emitters (40 nm)/1,3,5-tri(*m*-pyrid-3-yl-phenyl) benzene (TmPyPB) (40 nm)/LiF (1 nm)/Al (100 nm) were fabricated. The emissive layer is composed of a film consisting of 50 wt% emitter in mCP of **MR-D1** (Device 1) and **MR-D2** (Device 2), respectively. The schematic diagram of the device structure together with energy level of each layer is shown in Figure 5A. The electroluminescence (EL) spectra of the devices are presented in Figure 5B. The EL spectra of Device 2 is red-shifted compared to that of Device 1. The devices show sky-blue to green emission, with λ_{EL} of 493 and 496 nm (FWHM of 27 nm for each device) and Commission Internationale de L'Éclairage (CIE) coordinates of (0.12, 0.52) and (0.13, 0.54), respectively. The trends in EL match those observed in the PL spectra in both toluene and 1 wt% PMMA film, indicating that there is little aggregation occurring in the neat film. The density-voltage-luminance (J-V-L) curves for both devices are shown in Figure 5C. Both Devices 1 and 2 possess very low turn-on voltages of 3.3 V. Figure 5D shows the EQE versus current density for both devices. The EQE_{max} of Devices 1 and 2 are 27.7% and 21.0%, respectively, which are quite comparable to our previously reported **tBuCz2m2pTRZ** dendrimer OLED (EQE_{max} = 28.7%). The EQE_{max} values were obtained at 890 and 1074 cd/m², which reflect the very low efficiency roll-off at 1000 cd/m² of around 4% (EQE₁₀₀₀ of 26.8%) for Device 1, and at 2000 cd/m² at around 19% and 30% (EQE₂₀₀₀ of 22.3% and 14.7%) for Devices 1 and 2, respectively. The efficiency roll-off is much lower than that of the OLED with **tBuCz2m2pTRZ** where at 500 cd/m² the efficiency roll-off was 14% (EQE₅₀₀ of 22.7%).⁷ While the reported device with **tBuCz2m2pTRZ** showed a λ_{EL} of 540 nm, the emission was broad in the host-free device (FWHM of 97 nm), and the corresponding CIE coordinates were (0.37, 0.57). In the present work, the emission profile is narrower, with FWHM of 27 nm for both Devices 1 and 2.

3 | CONCLUSION

We have reported preliminary photophysical characterization and device performance of one of the first MR-TADF based dendrimer emitter **MR-D1** and a reference small molecule emitter **MR-D2**. **MR-D1** and **MR-D2** both show narrowband sky-blue emission at 490 and 495 nm with FWHM of 23 and 29 nm. Their small ΔE_{ST} is 0.14 and 0.13 eV and their delayed lifetime τ_d of 159 and 91 μs , respectively, in PMMA matrix at 1 wt% concentration reflect the MR-TADF character of these emitters. The solution-processed OLEDs based on **MR-D1** show high EQE_{max} of 27.7% and narrowband sky-blue EL emission of 493 nm with FWHM of 27 nm. Notably,

the efficiency roll-off at 2000 cd/m² is quite low with EQE₂₀₀₀ of 22.3%. This report demonstrates how solution-processed OLEDs can show both high EQE and narrowband emission.

ACKNOWLEDGMENTS

Sen Wu thanks the China Scholarship Council (201906250199). Dianming Sun acknowledges support from the Royal Academy of Engineering Enterprise Fellowship (EF2122-13106). Eli Zysman-Colman acknowledges support from Engineering and Physical Sciences Research Council (EPSRC; EP/L017008, EP/P010482/1).

ORCID

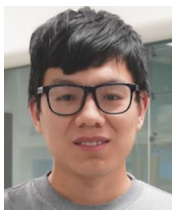
Eli Zysman-Colman  <https://orcid.org/0000-0001-7183-6022>

REFERENCES

1. Tang CW, VanSlyke SA. Organic electroluminescent diodes. *Appl Phys Lett*. 1987;51(12):913–915. <https://doi.org/10.1063/1.98799>
2. Forrest SR. The path to ubiquitous and low-cost organic electronic appliances on plastic. *Nature*. 2004;428(6986):911–918. <https://doi.org/10.1038/nature02498>
3. Friend RH, Gymer R, Holmes A, Burroughes J, Marks R, Taliani C, et al. Electroluminescence in conjugated polymers. *Nature*. 1999;397(6715):121–128. <https://doi.org/10.1038/16393>
4. Kim H, Byun Y, Das RR, Choi B-K, Ahn P-S. Small molecule based and solution processed highly efficient red electrophosphorescent organic light emitting devices. *Appl Phys Lett*. 2007;91(9):093512. <https://doi.org/10.1063/1.2776016>
5. Xie Y, Li Z. Thermally activated delayed fluorescent polymers. *J Polym Sci, Part A: Polym Chem*. 2017;55(4):575–584. <https://doi.org/10.1002/pola.28448>
6. Wu S, Liu H, Sun W, Li X, Wang S. Regulation of peripheral tert-butyl position: approaching efficient blue OLEDs based on solution-processable hole-transporting materials. *Org Electron*. 2019;71:85–92. <https://doi.org/10.1016/j.orgel.2019.05.005>
7. Sun D, Duda E, Fan X, Saxena R, Zhang M, Bagnich S, et al. Thermally activated delayed fluorescent dendrimers that underpin high-efficiency host-free solution-processed organic light-emitting diodes. *Adv Mater*. 2022;(23):2110344. <https://doi.org/10.1002/adma.202110344>
8. Tao Y, Yuan K, Chen T, Xu P, Li H, Chen R, et al. Thermally activated delayed fluorescence materials towards the breakthrough of organoelectronics. *Adv Mater*. 2014;26(47):7931–7958. <https://doi.org/10.1002/adma.201402532>
9. Wong MY, Zysman-Colman E. Purely organic thermally activated delayed fluorescence materials for organic light-emitting diodes. *Adv Mater*. 2017;29(22):1605444. <https://doi.org/10.1002/adma.201605444>
10. Albrecht K, Matsuoka K, Fujita K, Yamamoto K. Carbazole dendrimers as solution-processable thermally activated delayed-fluorescence materials. *Angew Chem Int Ed*. 2015; 54(19):5677–5682. <https://doi.org/10.1002/anie.201500203>

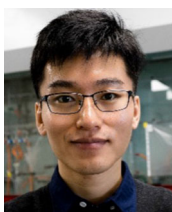
11. Liu Y, Li C, Ren Z, Yan S, Bryce MR. All-organic thermally activated delayed fluorescence materials for organic light-emitting diodes. *Nat Rev Mater*. 2018;3(4):18020. <https://doi.org/10.1038/natrevmats.2018.20>
12. Madayanad Suresh S, Hall D, Beljonne D, Olivier Y, Zysman-Colman E. Multiresonant thermally activated delayed fluorescence emitters based on heteroatom-doped nanographenes: recent advances and prospects for organic light-emitting diodes. *Adv Funct Mater*. 2020;30(33):1908677. <https://doi.org/10.1002/adfm.201908677>
13. Hatakeyama T, Shiren K, Nakajima K, Nomura S, Nakatsuka S, Kinoshita K, et al. Ultrapure blue thermally activated delayed fluorescence molecules: efficient HOMO–LUMO separation by the multiple resonance effect. *Adv Mater*. 2016; 28(14):2777–2781. <https://doi.org/10.1002/adma.201505491>
14. Connelly NG, Geiger WE. Chemical redox agents for organometallic chemistry. *Chem Rev*. 1996;96(2):877–910. <https://doi.org/10.1021/cr940053x>
15. Hall D, Sancho-Garcia JC, Pershin A, Ricci G, Beljonne D, Zysman-Colman E, et al. Modeling of multiresonant thermally activated delayed fluorescence emitters— properly accounting for electron correlation is key! *J Chem Theory Comput*. 2022; 18(8):4903–4918. <https://doi.org/10.1021/acs.jctc.2c00141>

AUTHOR BIOGRAPHIES



Sen Wugraduated from Wuhan Institute of Technology with a BS degree in Applied Chemistry. He then received his MSc in Chemistry from Tianjin University under the supervision of Professor Shirong Wang, where he mainly focused on

the design of hole-transporting materials. Now, he is in the final year of his PhD under the supervision of Prof. Eli Zysman-Colman at the University of St Andrews. His current research focuses on designing narrowband emission TADF emitters for organic light-emitting diodes.



Dianming Sun is currently a Royal Academy of Engineering Enterprise fellow at the University of St Andrews. He received his Ph.D. from the Beijing University of Chemical Technology in 2016 under the supervision of Prof. Zhongjie Ren and

Prof. Shouke Yan. After that, he moved to the University of St Andrews with the support from the National

Postdoctoral Program for Innovative Talents and focused on developing thermally activated delayed fluorescence (TADF) dendrimers. In 2019, he was then awarded a prestigious Marie Skłodowska-Curie Fellowship by the European Commission under the Horizon 2020 framework. His research interests cover molecular design, synthesis, photophysics, and organic light-emitting diodes (OLEDs) fabrication.



Eli Zysman-Colman obtained his Ph.D. from McGill University in 2003 under the supervision of Prof. David N. Harpp as an FCAR scholar, conducting research in physical organic sulfur chemistry. He then completed two postdoctoral fellowships, one in

supramolecular chemistry with Prof. Jay Siegel at the Organic Chemistry Institute, University of Zurich as an FQRNT fellow and the other in inorganic materials chemistry with Prof. Stefan Bernhard at Princeton University as a PCCM fellow. He joined the department of chemistry at the Université de Sherbrooke in Quebec, Canada as an assistant professor in 2007. In 2013, he moved to the University of St Andrews in St Andrews, UK, where he is presently Professor of Optoelectronic Materials, a Fellow of the Royal Society of Chemistry and a past holder of a Royal Society Leverhulme Trust Senior Research Fellowship. His research program focuses on the rational design of: (I) luminophores for energy-efficient visual displays and flat panel lighting based on OLED and light-emitting electrochemical cell (LEEC) device architectures; (II) sensing materials employed in electrochemiluminescence; and (III) photocatalyst developing for use in organic reactions.

How to cite this article: Wu S, Sun D, Zysman-Colman E. Solution-processed high-performance organic light-emitting diodes containing a green-emitting multiresonant thermally activated delayed fluorescent dendrimer. *J Soc Inf Display*. 2023. <https://doi.org/10.1002/jsid.1204>